NeuroImage 57 (2011) 885–891

Contents lists available at ScienceDirect

NeuroImage

journal homepage: www.elsevier.com/locate/ynimg

Neuroplastic changes following rehabilitative training correlate with regional electrical field induced with tDCS

M.A. Halko [a], A. Datta [c], E.B. Plow [b], J. Scaturro [c], M. Bikson [c], L.B. Merabet [d,*]

[a] The Berenson-Allen Center for Noninvasive Brain Stimulation, Department of Neurology, Beth Israel Deaconess Medical Center, Harvard Medical School, Boston, MA, USA
[b] Department of Biomedical Engineering, Lerner Research Institute, Physical Medicine and Rehabilitation, The Cleveland Clinic Foundation, Cleveland, OH, USA
[c] Department of Biomedical Engineering, The City College of New York of CUNY, New York, NY, USA
[d] Vision Rehabilitation Center, Department of Ophthalmology, Massachusetts Eye and Ear Infirmary, Harvard Medical School, Boston, MA USA

ARTICLE INFO

Article history:
Received 24 February 2011
Revised 6 May 2011
Accepted 7 May 2011
Available online 18 May 2011

ABSTRACT

Transcranial direct current stimulation (tDCS) has recently emerged as a promising approach to enhance neurorehabilitative outcomes. However, little is known about how the local electrical field generated by tDCS relates to underlying neuroplastic changes and behavior. To address this question, we present a case study analysis of an individual with hemianopia due to stroke and who benefited from a combined visual rehabilitation training and tDCS treatment program. Activation associated with a visual motion perception task (obtained by functional magnetic resonance imaging; fMRI) was used to characterize local changes in brain activity at baseline and after training. Individualized, high-resolution electrical field modeling reproducing precise cerebral and lesioned tissue geometry, predicted distortions of current flow in peri-lesional areas and diffuse clusters of peak electric fields. Using changes in fMRI signal as an index of cortical recovery, correlations to the electrical field map were determined. Significant correlations between the electrical field and change in fMRI signal were region specific including cortical areas under the anode electrode and peri-lesional visual areas. These patterns were consistent with effective tDCS facilitated rehabilitation. We describe the methodology used to analyze tDCS mechanisms through combined fMRI and computational modeling with the ultimate goal of developing a rationale for individualized therapy.

© 2011 Elsevier Inc. All rights reserved.

Introduction

Transcranial Direct Current Stimulation (tDCS) alters cortical excitability by passing current between electrode pads placed on the overlying surface of the scalp (Antal et al., 2003; Nitsche and Paulus, 2000). Acute modulatory effects in excitability can last minutes to hours and repeated stimulation sessions can lead to still longer-lasting effects (Boggio et al., 2007, 2008; Ferrucci et al., 2009; Fregni et al., 2006; Lindenberg et al., 2010; Rigonatti et al., 2008). tDCS is clinically attractive due to its relatively noninvasive nature, good safety profile, and ease of implementation (Nitsche et al., 2008; Priori, 2003; Williams et al., 2009). The ability to generate sustained changes in excitability (i.e. promote underlying neuroplastic changes) and the fact that tDCS can be delivered in combination with behavioral tasks, has rendered this technique very appealing in terms of potentially enhancing neurorehabilitative outcomes (Bolognini et al., 2009; Schlaug and Renga, 2008; Williams et al., 2009).

Typically, positioning of the anode electrode over the targeted cortical region (i.e. "anodal stimulation") is associated with up-regulating cortical excitability while the cortical region under the cathode electrode ("cathodal stimulation"), is associated with down-regulation (Nitsche and Paulus, 2000). However, overall pattern of current flow within the brain is broad and complex reflecting physiological and potential pathophysiological subtleties of morphology. For example, the presence of highly-conductive cerebral spinal fluid (CSF) in the ventricles and in lesions (e.g. from stroke), greatly alters how current in distributed in surrounding neural tissue (Datta et al., 2009; Wagner et al., 2007). Moreover, for a fixed anode electrode location, simply varying the position of the "return" (cathode) electrode can profoundly influence overall current distribution and thus brain activity (Baudewig et al., 2001; Cogiamanian et al., 2007; Elbert et al., 1981; Moliadze et al., 2010; Nitsche and Paulus, 2000; Priori et al., 2008). Due to the complexity of stimulation parameter space and intersubject variability, computational models are becoming increasingly valued to predict brain current flow during tDCS (Datta et al., 2009, 2010; Im et al., 2008; Miranda et al., 2006; Wagner et al., 2007). However, neurophysiological mechanisms that underlie behavioral changes (for example, as the result of prolonged rehabilitative training) are complex and brain current flow does not simply map to any behavioral outcome. Thus, there remain fundamental questions as how to interpret and leverage these models of brain current flow in order to optimize, and potentially customize, tDCS on an individual basis.

* Corresponding author.
E-mail address: lotfi_merabet@meei.harvard.edu (L.B. Merabet).

1053-8119/$ – see front matter © 2011 Elsevier Inc. All rights reserved.
doi:10.1016/j.neuroimage.2011.05.026

Most measurements of neurobiological change induced by tDCS have focused on correlating stimulus parameters such as current intensity and duration with changes in task performance or evoked potentials (Antal et al., 2006; Nitsche et al., 2008; Nitsche and Paulus, 2000, 2001). While these physiological changes are thought to be measures of underlying cortical plasticity, characterizing whole-brain and task related neuroplastic changes could be carried out using advanced neuroimaging methodologies such as functional magnetic resonance imaging (fMRI) (Ward et al., 2003). Moreover, combining fMRI and computational modeling then allows consideration of how regional current flow relates to functional changes.

Here, we combined fMRI to characterize regional changes in brain activity with an individualized, high-resolution computational model of brain current flow in a patient who underwent a successful combined visual rehabilitation and tDCS training protocol. Specifically, we evaluated correlations between estimates of electrical field and fMRI signal change related to underlying brain activity. Two scenarios of interest were pursued: 1) an analysis predicting changes occurring directly underneath the stimulation electrodes, and 2) an analysis predicting areas of the highest electrical field generated by tDCS. To our knowledge, this study provides the first report demonstrating correlative effects of regional brain current flow during tDCS with brain activity characterized by fMRI.

Methods

Patient and rehabilitation (tDCS and visual training)

At the time of study, patient RM was a 61 year old right-handed female diagnosed with a right homonymous hemianopia following a left posterior cerebral artery stroke (chronic phase: post-lesion duration of 72 months). Evaluation of structural MRI images revealed mild encephalomalacia and gliosis. Automated visual perimetry testing confirmed a dense right homonymous field deficit (greater in the inferior field) with macular sparing. At the time of study, the patient was assessed as neurologically and cognitively normal, with the exception of the hemianopia. The patient's visual acuity was 20/20 (with correction) in both eyes. The patient had no metal implants in the head or any other contra-indications precluding her from participating in the study. The patient provided written informed consent and the study was approved by the investigational review board of Beth Israel Deaconess Medical Center and carried out in accordance to the tenants of the Declaration of Helsinki.

As part of her rehabilitative training, patient RM underwent 3 months (2 half-hour sessions, 3 days a week) of Visual Restoration Therapy (VRT; NovaVision Inc, Boca Raton, FL, USA) combined with concurrent tDCS carried out in a controlled laboratory setting (36 total visits). For complete details regarding VRT, see Kasten et al. (1998). Briefly, the patient was seated comfortably in front of a computer screen and constant viewing distance. Under binocular viewing conditions, she was instructed to detect and respond (using a key-press) a series of light stimuli presented primarily within the border between the areas of affected and unaffected vision (referred to as the "transition zone"). During each half-hour session, approximately 500 light stimuli were presented (size varying systematically between 1.5° and 0.5°, presentation time of 2000 ms, luminance ranging from <1 cd/m^2 to 50 cd/m^2). Previous studies have shown that visual training of this region leads to a significant expansion of the visual field border (5° on average) following 6 months of daily training (Kasten et al., 1998).

In conjunction to visual rehabilitation training, tDCS was delivered concurrently using an electrode configuration designed to upregulate occipital cortex excitability and known to enhance visuo-perceptual functioning in healthy participants (Antal et al., 2004, 2003; Kraft et al., 2010). For this purpose, two electrode sponges (5×7 cm; 35 cm^2 surface area, soaked in 0.9% saline) were used with the anode electrode placed overlying the Oz position and the reference (cathode) electrode placed over Cz (vertex) following the 10–20 International EEG coordinate system. Note that with this electrode configuration, the anode and cathode electrodes were positioned along the mid-line so as to stimulate bilaterally both the lesioned and non-lesioned hemispheres. The electrodes were then connected to a battery operated unit delivering continuous current (2 mA; IOMED Inc., Salt Lake City, UT) for the entire duration of VRT training. Current was delivered continuously throughout the 30 minute training sessions with a ramping up and down period each lasting approximately 30 s. Electrodes were secured in place using non-latex rubber straps.

fMRI and visual task

The patient underwent two fMRI sessions; one during the first week and the second after the 3 month training period. A high-resolution anatomical T1 weighted image was collected (MPRAGE; 1 mm^3) using a 3 T Phillips scanner equipped with an 8 channel head coil. Four 368 s fMRI runs were collected (axial slices; 3 mm^2 in-plane resolution; 3 mm slice thickness; 1 mm gap; 28 ms TE; 2000 ms TR; 90° flip angle). The visual stimulus task of interest was comprised of random dot kinetograms (visual extent of 4×4°) presented within the area of visual training, i.e. the transition zone region bordering between the blind and intact visual field. Kinetograms were presented in blocks of 20 s with alternating rest periods of 8 s. The visual stimulus was presented such that 70% of the dots moved in a single coherent direction (30% of the dots moved in random directions). The subject performed a behavioral alternative forced choice task in which two kinetograms were presented one after another. Each kinetogram was presented for 500 ms, with a 250 m inter-stimulus interval. One trial (two kinetogram presentations) was performed every 4 s with a maximal response time of 2750 ms. The task was to indicate (using a key press) whether or not the pair matched in direction of motion. The difference between the radial directions was manipulated and set at an a priori defined threshold of 75% accuracy so as to ensure that visual stimulation was equivalent and the attentional demands were matched across scanning sessions. Thresholds were determined prior to the scanning session using a fixed-staircase design to indentify the 50% threshold, and then followed by 10 to 50 trials at various levels above threshold to identify the 75% correct performance level. Performance was slightly worse during scanning sessions (mean pre-test performance: 49% and mean post-test performance: 58%. Not significantly different; t-test; $p=0.37$).

FMRI data processing was carried out using FEAT (FMRI Expert Analysis Tool) Version 5.98, part of FSL software package (FMRIB's Software Library, www.fmrib.ox.ac.uk/fsl). The following pre-processing was applied: motion correction (Jenkinson et al., 2002), non-brain removal (Smith, 2002), spatial smoothing using a Gaussian kernel of FWHM 5 mm, grand-mean intensity normalization of the entire 4D dataset by a single multiplicative factor, and high-pass temporal filtering (Gaussian-weighted least-squares straight line fitting, with sigma = 50.0 s). Activation for each block of kinetograms was entered into a general linear model (GLM) which included head motion nuisance regressors. Higher-level analysis between pre-treatment and post-treatment was carried out using a fixed effects model, that is, by forcing the random effects variance to zero in FLAME (FMRIB's Local Analysis of Mixed Effects) (Beckmann et al., 2003; Woolrich, 2008; Woolrich et al., 2004).

Electric field model

The individualized head model was created from the T1-weighted MRI scans of the patient. Using a combination of tools from the FSL and Simpleware (Exeter, UK), the patient's head was segmented into compartments representing gray matter, white matter, cerebrospinal fluid (CSF), skull, scalp, eye region, muscle, air, and blood vessels

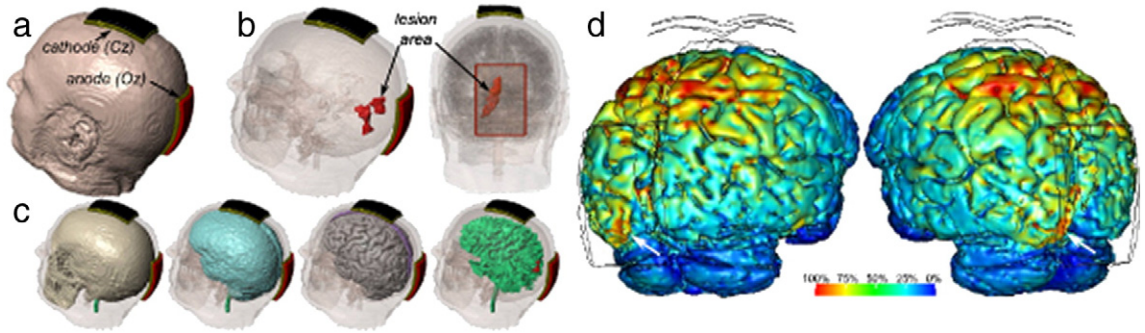

Fig. 1. Construction of patient-specific cortical electrical field model. (a) tDCS pads were placed with the anode electrode over the occipital pole (Oz) and cathode overlying the vertex (Cz) (b) the patient's occipital lesion (filled in red) was located with the left hemisphere along the upper and lower banks of the calcarine sulcus. Note that the anode electrode was positioned along the midline to stimulate both the intact and lesioned hemispheres and encompassed the entire lesioned area (see electrode outline in posterior view). (c) Selected compartments from the finite element method (FEM) model (from left to right: skull, meninges, gray matter, white matter). (d) Posterior views of cortical tDCS electrical field map. The white arrow indicates an area of higher regional electrical field corresponding to the lesioned left hemisphere.

(Custom Segmentation, Soterix LLC, NY, USA; see Fig. 1). The lesion site was classified as CSF (Wagner et al., 2007; Datta et al., 2010). The finite element (FE) mesh generated from the segmentation masks was exported to COMSOL Multiphysics 3.5a (Burlington, MA) for computation of electric fields.

We modeled the electrode configuration used in this study such that anode electrode was located at Oz and the cathode electrode was at Cz (Fig. 1). The stimulation electrodes were modeled as 7×5 cm sponge-based electrodes and current densities corresponding to 2 mA total current were applied. The following isotropic electrical conductivities (in S/m) were assigned; gray matter: 0.276; white matter: 0.126; eye region: 0.4; CSF: 1.65; skull: 0.01; scalp: 0.465; air: 1e-15; sponge: 1.4; electrode: 5.8e7 (Datta et al., 2009; Nadeem et al., 2003; Wagner et al., 2007). The muscle and blood vessel compartments were assigned the conductivity of scalp tissue. The Laplace equation was solved and induced cortical electric field (EF) magnitude maps for the electrode configuration was determined (Figs. 1 and 2).

Combining electric field maps and fMRI activation maps

The cortical surface electrical field magnitude maps were then resampled into the same volumetric space as the fMRI data for direct voxelwise comparisons. To assess the correlations between fMRI-derived changes in activation and electrical field magnitude, regions of interest (ROIs) were drawn on the cortical surface. These anatomical regions were defined by a sphere intersecting the cortical gray matter. Six regions of interest were drawn: left and right occipital pole, left and right medial calcarine sulcus, left superior parietal and left vertex. These ROIs were chosen based on the following rationale. First, the occipital pole and vertex measures corresponded to the locations of the tDCS electrodes. Second, based on current modeling, the parietal cortex was predicted to be the area of highest increase in electrical field (see Fig. 1). Finally, the calcarine sulcus was chosen based on prior studies suggesting that peri-lesional areas were the site of potential neuroplastic changes related to the recovery of visual field function following VRT training (Kasten et al., 1998; Pleger et al., 2003).

Results

Following combined visual rehabilitative training and tDCS, patient RM exhibited a visual border increase of approximately 4°. Despite employing a protracted training regimen (3 months compared to the typical 6), the improvement observed was in accordance to previous studies describing the beneficial effects VRT (Kasten et al., 1998). Given that tDCS had likely facilitated the observed recovery of visual function (Plow et al., 2009), we hypothesized that a correspondence would exist between the brain current flow (regional electric field) generated by tDCS and areas responsible for the visual recovery observed. On the motion perception task, her 75% threshold measure for discriminating changes in orientation of 70% coherent dots improved from 70° pre-test to 60° post-test.

Fig. 1d shows the predicted cortical electric field of the patient as a result of tDCS and based on the electrode montage used in this study. Visual inspection revealed a pattern of relatively high electrical field across the parietal cortex bilaterally (located between the anode and cathode electrodes) as well as in peri-lesional areas (see also Fig. 2). Furthermore, while both electrodes were placed along the midline of the scalp, the electrical field was markedly higher in left occipital cortex near the lesion compared to the corresponding right hemisphere location.

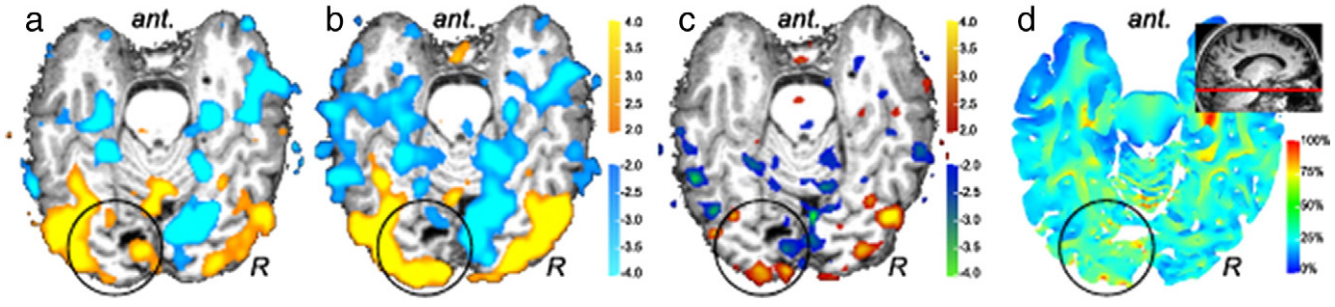

Fig. 2. FMRI activation patterns in response to a visual detection task (random dot kinetograms presented in the transition zone of the visual filed) shown on axial slice projection. The contrast of task activation (yellow) vs rest (blue) is shown at (a) baseline and (b) post-treatment timepoint. (c) Difference map showing activation associated with post-treatment (red) vs baseline (blue). (d) Corresponding FEM-predicted electrical field from tDCS highlights localized areas of peak field with areas of the occipital pole and peri-lesional areas. Inset figure illustrates relative location of axial slice.

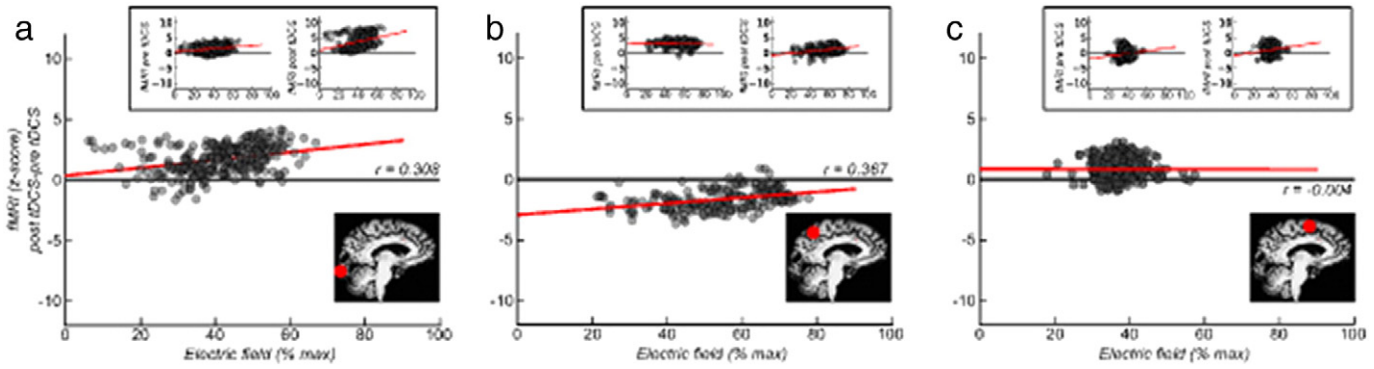

Fig. 3. Regional correlations between electrical field and change in fMRI activity. (a) Correlation of individual voxel electrical field and fMRI change in signal for gray matter underneath the anode at the ipsilesional occipital pole. Inset left: correlation between baseline fMRI activation and electrical field; inset right: correlation between post-treatment fMRI activation and electrical field. (b) Correlations of voxels in ipsilesional parietal cortex. Inset left, correlation between baseline fMRI activation and electrical field; Inset right, correlation between post-treatment fMRI activation and electrical field. (c) Correlations of voxels at ipsilesional vertex. Inset left, correlation between baseline fMRI activation and electrical field; Inset right, correlation between post-treatment fMRI activation and electrical field.

The primary impetus of the study was to compare the change in brain activation patterns following treatment (assessed with fMRI) with a map of electrical field in the brain. Activation maps for visual random-dot kinetograms compared to rest were generated (Fig. 2). Within-session activation maps were created for baseline (Fig. 2a), and post-treatment (i.e. combined VRT and tDCS; Fig. 2b). At both timepoints, activation within extrastriate visual areas was observed. However, perilesional activation (observed at the baseline) was not observed at the post-treatment timepoint. In contrast, no activation was observed within the occipital pole at baseline. However, at post-treatment, activation was observed within the occipital pole. This shift of activation is summarized in an across-sessions difference map where the baseline activation map is contrasted with the post-treatment activation map (Fig. 2c). Qualitative examination of the electrical field map (Fig. 2d) suggests that areas of the occipital pole showed increased activation following treatment that was similar in location to that of the locally higher electrical field.

In order to quantify the relationship between local electrical field and changes in activation from baseline to post-treatment, we examined correlations between electrical field and changes in activation across sessions within gray matter regions of interest. At each region of interest location, a given voxel has an electrical field value and corresponds to a change in activation value (difference between post-treatment and baseline). The correlation was then computed for all voxels within a given region of interest. Current models of tDCS-induced cortical plasticity emphasize changes in cortical activity occurring directly beneath the stimulation pads. We initially assessed the relationship between change in fMRI activation and electrical field by examining regions of interest in the ipsilesional hemisphere underneath the anode electrode at Oz (occipital pole) and cathode electrode at Cz (vertex) as well as in between the electrodes

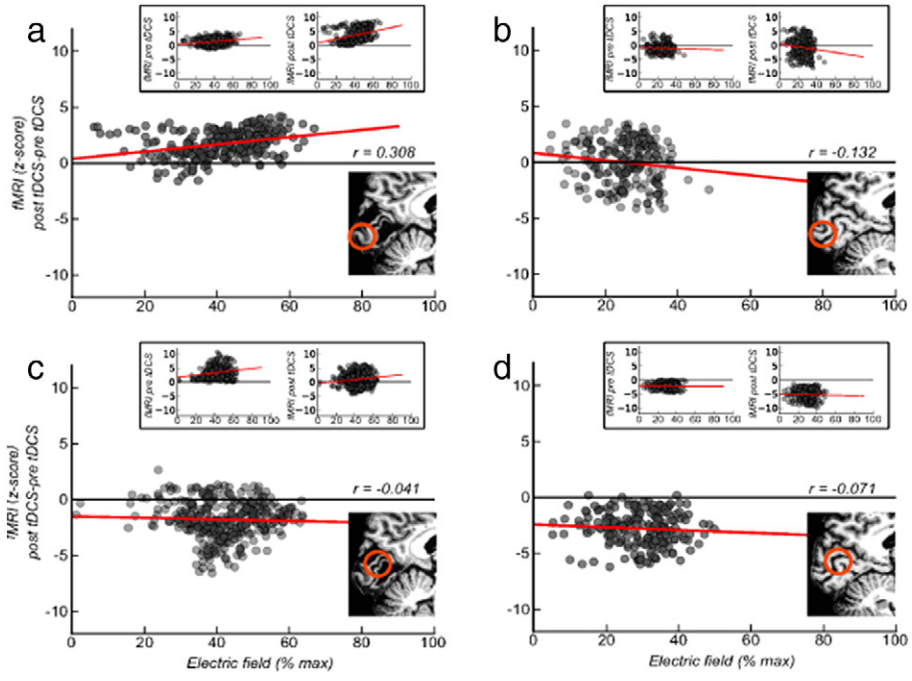

Fig. 4. Regional correlations between electric field and change in fMRI activity in the occipital lobe. (a) Correlation of individual voxel electric field and fMRI signal difference between post-treatment and baseline at the lesioned occipital pole. Inset left, correlation between fMRI signal at baseline and electric field; Inset right correlation between fMRI signal at post-treatment and electric field. (b) Correlations between electric field and fMRI at intact occipital pole. (c) Correlations between electric field and fMRI at lesioned calcarine sulcus. (d) Correlations between electric field and fMRI at the intact calcarine sulcus.

in parietal cortex (Fig. 3). Increased fMRI activation post-treatment compared to pre-treatment was accompanied by greater electrical field at the occipital pole ($r = 0.31$; $t(247) = 5.09$; $p < 0.05$) and in parietal cortex ($r = 0.37$; $t(185) = 5.37$; $p < 0.05$). No change in fMRI activation across sessions was observed to correspond with electrical field at the vertex site ($r = 0.00$; $t(236) = -0.06$; $p = 0.95$).

Recovery of visual function has been previously associated with changes in activity occurring within perilesional areas of the visual cortex (Eysel and Schweigart, 1999; Glassman, 1971; Pleger et al., 2003). In order to assess correspondence between electrical field and change in cortical activation, additional regions of interest were drawn on gray matter at the ipsilesional occipital pole, contralesional occipital pole, ipsilesional perilesional calcarine sulcus, and a corresponding contralesional calcarine sulcus location (Fig. 4). As reported above, change in fMRI signal was positively correlated with electrical field at the ipsilesional occipital pole. A non-significant negative correlation was found on the contralesional occipital pole ($r = -0.13$, $t(200) = -1.88$, $p = 0.06$). Despite regionally larger electrical field in perilesional calcarine sulcus, there were no significant correlations between electrical field and activation change within perilesional calcarine sulcus ($r = -0.04$, $t(323) = -0.04$, $p = 0.47$). Contralesional calcarine sulcus also did not show a correlation between electrical field and change in fMRI activation ($r = -0.07$, $t(195) = -0.99$, $p = 0.32$).

Discussion

We demonstrate the relationship between predicted regional current flow resulting from prolonged tDCS and changes in functional activation (assessed by fMRI) in a patient undergoing a successful combined visual rehabilitation and tDCS therapy program. Consistent with previous computer model descriptions, tDCS delivered with relatively large electrodes resulted in diffuse electrical activation in regions under and between electrodes and with local clustering of "hot spots" of current, most notably within perilesional areas (Datta et al., 2009; Wagner et al., 2007). The local clustering surrounding perilesional areas is believed to be due to "funneling" effects related to the highly-conductive milieu surrounding lesion tissue (Datta et al., 2009; Holdefer et al., 2006). This could be interpreted as fortuitous, as this lesioned region (and the occipital cortical pole in general) was the intended target for visual rehabilitative training and hence the initial rationale for delivering anodal tDCS to up regulate excitability in this area. Change in fMRI signal following tDCS and rehabilitative treatment was found near the anodal pad on the occipital pole consistent with previous reports of fMRI signal change following acute tDCS or acute transcranial random noise stimulation (Baudewig et al., 2001; Chaieb et al., 2009; Jang et al., 2009; Kwon et al., 2008).

Though there is a rational basis for a mechanistic link between electrically activated regions and changes in brain activity (see below), it is important to acknowledge that the fMRI/model correlation shown does not prove causality. One may consider repeating this analysis with the addition of a control (i.e. sham-stimulation) and/or a tDCS only subject to help disentangle the causal effects of the stimulation. However, several points need to be considered. First, inter-individual variability (such as lesion type, extent, and location) are all likely to further confound the possibility of a valid comparison based on stimulation status alone. Second, *both* the effects of tDCS *and* the visual rehabilitation training employed may have contributed to the underlying neuroplastic changes (and associated correlations with electrical field) observed here. However, their respective contributions cannot be disentangled at this time. In order to accurately characterize and correlate the effects related to tDCS over time, one would have to obtain comparative fMRI activation data from patients undergoing tDCS alone. While this could potentially permit disentangling the effect of tDCS, ethically, long term passive stimulation of a patient for this purpose could not be justified. Finally, there remains the fact that "sham tDCS" cannot in of itself be mathematically modeled in order to allow for site-specific correlative analysis in the way that we have demonstrated here. Another (perhaps more robust) possibility to consider would be to compare correlations between fMRI task-related activation and tDCS modeling characterizing a different electrode montage (e.g. reversing the anode and cathode position or using a bilateral occipital electrode montage) in the *same patient*. While this may allow for drawing stronger causal conclusions, logistically it was not feasible due to the pre-defined and prolonged clinical treatment protocol that had to be carried out. It is for this reason that we employed a within-patient correlative approach comparing observed changes in activation with generated electrical field over time. These issues notwithstanding, the nature of observed correspondences between stimulated regions and neuroplastic changes (including dependencies on success of rehabilitation training, stimulation polarity as well as region function pathology) provides an initial substrate for considering how the spatial distribution of current reflects behavioral outcomes. Future studies comparing normal controls and patients with real and sham stimulation conditions (i.e. factorial study designs) and under acute and long-term stimulation should be performed. Addressing the broader relationship between electric field and neuroplasticity is fundamental to the understanding and advancement of tDCS as a viable therapeutic possibility.

FMRI is a useful outcome measure for characterizing underlying changes related to neuroplasticity (Ward et al., 2003). When combined with a predictive model of electrical field, it is possible to better characterize the mechanism of action of tDCS. Animal studies have shown that weak direct currents induce cortical facilitation or suppression depending on the utilization of anodal or cathodal stimulation (Bindman et al., 1964; Gartside, 1968). In humans, tDCS shows a similar pattern of facilitation and suppression (Nitsche and Paulus, 2000). It has been inferred that the critical component of tDCS is local polarization of cortical tissue. However, it is not clear which components of the electric field are most predictive of behavioral outcomes, how they contribute to enhancing rehabilitative effects, or how they correlate with underlying neuroplastic changes at the level of the brain. The current view in the literature is that cortical excitability underneath the anodal pad is facilitated while it is suppressed underneath the cathodal electrode pad (Nitsche et al., 2008). However, computer modeling suggests that the electric field is not evenly distributed under and between the pads, nor is it omnidirectional (Bikson et al., 2010). The distribution of field strength, polarity and directionality is likely to play important roles in neural modulation and deserve further careful investigation. Critically, all current tDCS montage positions assume the mechanism of action is directly under the electrode pads. This predicted mechanism of action can be assessed with improved modeling and specifically testing predictions where electric field density is kept the same across the expected regions of plastic changes, but manipulating other factors such as current directionality.

Cortical plasticity induced by tDCS is believed to be activity-dependant (Nitsche et al., 2007) and our results are in agreement with this view. For example, no decrease in fMRI activity was found at the vertex; the site of the cathodal electrode. It can be presumed that cortical regions directly under the cathode (vertex) are likely not involved in the processing random-dot kinetograms despite the suppressive effect of stimulation at that site. For this reason, calculated electric field maps from a particular montage must be assessed along with a predicted model of cortical function. Without a model of desired and targeted neurophysiological change, an estimation of electrical field in the brain will not, by itself, inform the clinical application of tDCS.

There are other limitations to our approach that need to be addressed. While this is a single case-study report, continued studies implicating the approach described here (as well as other forms of

neuroimaging) can help better understand the relationship between changes in cortical activity and local electrical field generated by electrical stimulation. From an analysis perspective, future studies could incorporate automated segmentation procedures to reduce manual effort (as was necessary here), and allow for more efficient estimation of local cortical electrical field maps as a function of different electrode parameters. It should be stressed that repeated application of tDCS to facilitate recovery of cortical function is likely an individualized process. The nature of cortical injury suggests that different injuries will lead to different models of recovery. For example, recovery of motor function after stroke is associated with a number of factors such as lesion location, extent, and the ability of the activity of the contralesional motor cortex (Stinear, 2010; Ward et al., 2003). Secondly, it is important to note that fMRI is typically a subtractive function and does equate to observing absolute cortical activity. Therefore, it is highly dependent on the task and analysis contrasts chosen that may in turn influence the patterns of fMRI activation observed. To mitigate this latter issue, we adjusted visual task difficulty such that performance was maintained at 70% across scanning sessions in order to alleviate potential changes in task performance strategy during the 3 month training period. Within subject error on simple visual task activation was on the order of 3 mm (Peelen and Downing, 2005), and our observed shift of activity to the occipital pole was approximately 15 mm. This suggests that this shift represents a change in cortical activity function and is not a product of repeated testing.

In conclusion, we have developed a technique to directly investigate changes in cortical activity associated with a combined tDCS and visual rehabilitation training program in relation to generated electrical field. We have found that electrical field maps are correlated with functional changes assessed with fMRI. This technique can be directly applied to future studies to establish which components of the electrical field influence modulatory effects of tDCS. Resolving the relationship of individual field differences and neural plasticity may also have important clinical utility in developing appropriate individual tDCS montages so as to improve neurorehabiliative outcomes and recovery.

Acknowledgments

This work was supported by an investigator-initiated pilot grant from Novavision VRT Inc. and by the National Institutes of Health (K23-EY016131 to LBM).

References

Antal, A., Kincses, T.Z., Nitsche, M.A., Paulus, W., 2003. Manipulation of phosphene thresholds by transcranial direct current stimulation in man. Exp. Brain Res. 150, 375–378.

Antal, A., Kincses, T.Z., Nitsche, M.A., Bartfai, O., Paulus, W., 2004. Excitability changes induced in the human primary visual cortex by transcranial direct current stimulation: direct electrophysiological evidence. Invest. Ophthalmol. Vis. Sci. 45, 702–707.

Antal, A., Nitsche, M.A., Paulus, W., 2006. Transcranial direct current stimulation and the visual cortex. Brain Res. Bull. 68, 459–463.

Baudewig, J., Nitsche, M.A., Paulus, W., Frahm, J., 2001. Regional modulation of BOLD MRI responses to human sensorimotor activation by transcranial direct current stimulation. Magn. Reson. Med. 45, 196–201.

Beckmann, C.F., Jenkinson, M., Smith, S.M., 2003. General multilevel linear modeling for group analysis in FMRI. Neuroimage 20, 1052–1063.

Bikson, M., Datta, A., Rahman, A., Scaturro, J., 2010. Electrode montages for tDCS and weak transcranial electrical stimulation: role of "return" electrode's position and size. Clin. Neurophysiol. 121, 1976–1978.

Bindman, L.J., Lippold, O.C., Redfearn, J.W., 1964. The action of brief polarizing currents on the cerebral cortex of the rat (1) during current flow and (2) in the production of long-lasting after-effects. J. Physiol. 172, 369–382.

Boggio, P.S., Nunes, A., Rigonatti, S.P., Nitsche, M.A., Pascual-Leone, A., Fregni, F., 2007. Repeated sessions of noninvasive brain DC stimulation is associated with motor function improvement in stroke patients. Restor. Neurol. Neurosci. 25, 123–129.

Boggio, P.S., Rigonatti, S.P., Ribeiro, R.B., Myczkowski, M.L., Nitsche, M.A., Pascual-Leone, A., Fregni, F., 2008. A randomized, double-blind clinical trial on the efficacy of cortical direct current stimulation for the treatment of major depression. Int. J. Neuropsychopharmacol. 11, 249–254.

Bolognini, N., Pascual-Leone, A., Fregni, F., 2009. Using non-invasive brain stimulation to augment motor training-induced plasticity. J. Neuroeng. Rehabil. 6, 8.

Chaieb, L., Kovacs, G., Cziraki, C., Greenlee, M., Paulus, W., Antal, A., 2009. Short-duration transcranial random noise stimulation induces blood oxygenation level dependent response attenuation in the human motor cortex. Exp. Brain Res. 198, 439–444.

Cogiamanian, F., Marceglia, S., Ardolino, G., Barbieri, S., Priori, A., 2007. Improved isometric force endurance after transcranial direct current stimulation over the human motor cortical areas. Eur. J. Neurosci. 26, 242–249.

Datta, A., Bansal, V., Diaz, J., Patel, J., Reato, D., Bikson, M., 2009. Gyri-precise head model of transcranial direct current stimulation: improved spatial focality using a ring electrode versus conventional rectangular pad. Brain Stimul. 2, 201–207 207 e201.

Datta, A., Bikson, M., Fregni, F., 2010. Transcranial direct current stimulation in patients with skull defects and skull plates: high-resolution computational FEM study of factors altering cortical current flow. Neuroimage 52, 1268–1278.

Elbert, T., Lutzenberger, W., Rockstroh, B., Birbaumer, N., 1981. The influence of low-level transcortical DC-currents on response speed in humans. Int. J. Neurosci. 14, 101–114.

Eysel, U.T., Schweigart, G., 1999. Increased receptive field size in the surround of chronic lesions in the adult cat visual cortex. Cereb. Cortex 9, 101–109.

Ferrucci, R., Bortolomasi, M., Vergari, M., Tadini, L., Salvoro, B., Giacopuzzi, M., Barbieri, S., Priori, A., 2009. Transcranial direct current stimulation in severe, drug-resistant major depression. J. Affect. Disord. 118, 215–219.

Fregni, F., Boggio, P.S., Nitsche, M.A., Marcolin, M.A., Rigonatti, S.P., Pascual-Leone, A., 2006. Treatment of major depression with transcranial direct current stimulation. Bipolar Disord. 8, 203–204.

Gartside, I.B., 1968. Mechanisms of sustained increases of firing rate of neurons in the rat cerebral cortex after polarization: reverberating circuits or modification of synaptic conductance? Nature 220, 382–383.

Glassman, R.B., 1971. Recovery following sensorimotor cortical damage: evoked potentials, brain stimulation and motor control. Exp. Neurol. 33, 16–29.

Holdefer, R.N., Sadleir, R., Russell, M.J., 2006. Predicted current densities in the brain during transcranial electrical stimulation. Clin. Neurophysiol. 117, 1388–1397.

Im, C.H., Jung, H.H., Choi, J.D., Lee, S.Y., Jung, K.Y., 2008. Determination of optimal electrode positions for transcranial direct current stimulation (tDCS). Phys. Med. Biol. 53, N219–N225.

Jang, S.H., Ahn, S.H., Byun, W.M., Kim, C.S., Lee, M.Y., Kwon, Y.H., 2009. The effect of transcranial direct current stimulation on the cortical activation by motor task in the human brain: an fMRI study. Neurosci. Lett. 460, 117–120.

Jenkinson, M., Bannister, P., Brady, M., Smith, S., 2002. Improved optimization for the robust and accurate linear registration and motion correction of brain images. Neuroimage 17, 825–841.

Kasten, E., Wust, S., Behrens-Baumann, W., Sabel, B.A., 1998. Computer-based training for the treatment of partial blindness. Nat. Med. 4, 1083–1087.

Kraft, A., Roehmel, J., Olma, M.C., Schmidt, S., Irlbacher, K., Brandt, S.A., 2010. Transcranial direct current stimulation affects visual perception measured by threshold perimetry. Exp. Brain Res. 207, 283–290.

Kwon, Y.H., Ko, M.H., Ahn, S.H., Kim, Y.H., Song, J.C., Lee, C.H., Chang, M.C., Jang, S.H., 2008. Primary motor cortex activation by transcranial direct current stimulation in the human brain. Neurosci. Lett. 435, 56–59.

Lindenberg, R., Renga, V., Zhu, L.L., Nair, D., Schlaug, G., 2010. Bihemispheric brain stimulation facilitates motor recovery in chronic stroke patients. Neurology 75, 2176–2184.

Miranda, P.C., Lomarev, M., Hallett, M., 2006. Modeling the current distribution during transcranial direct current stimulation. Clin. Neurophysiol. 117, 1623–1629.

Moliadze, V., Antal, A., Paulus, W., 2010. Electrode-distance dependent after-effects of transcranial direct and random noise stimulation with extracephalic reference electrodes. Clin. Neurophysiol. 121, 2165–2171.

Nadeem, M., Thorlin, T., Gandhi, O.P., Persson, M., 2003. Computation of electric and magnetic stimulation in human head using the 3-D impedance method. IEEE Trans. Biomed. Eng. 50, 900–907.

Nitsche, M.A., Paulus, W., 2000. Excitability changes induced in the human motor cortex by weak transcranial direct current stimulation. J. Physiol. 527 (Pt 3), 633–639.

Nitsche, M.A., Paulus, W., 2001. Sustained excitability elevations induced by transcranial DC motor cortex stimulation in humans. Neurology 57, 1899–1901.

Nitsche, M.A., Roth, A., Kuo, M.F., Fischer, A.K., Liebetanz, D., Lang, N., Tergau, F., Paulus, W., 2007. Timing-dependent modulation of associative plasticity by general network excitability in the human motor cortex. J. Neurosci. 27, 3807–3812.

Nitsche, M.A., Cohen, L.G., Wassermann, E.M., Priori, A., Lang, N., Antal, A., Paulus, W., Hummel, F., Boggio, P.S., Fregni, F., Pascual-Leone, A., 2008. Transcranial direct current stimulation: state of the art 2008. Brain Stimul. 1, 206–223.

Peelen, M.V., Downing, P.E., 2005. Within-subject reproducibility of category-specific visual activation with functional MRI. Hum. Brain Mapp. 25, 402–408.

Pleger, B., Foerster, A.F., Widdig, W., Henschel, M., Nicolas, V., Jansen, A., Frank, A., Knecht, S., Schwenkreis, P., Tegenthoff, M., 2003. Functional magnetic resonance imaging mirrors recovery of visual perception after repetitive tachistoscopic stimulation in patients with partial cortical blindness. Neurosci. Lett. 335, 192–196.

Plow, E.B., Obretenova, S., Poggel, D.A., Halko, M.A., Kenkel, S., Jackson, M., Torun, N., Maguire, S.B., Pascual-Leone, A., Merabet, L.B., 2009. Neuro-visual Rehabilitation Combined with Noninvasive Brain Stimulation to Enhance Function in Hemianopia. American Neurological Association.

Priori, A., 2003. Brain polarization in humans: a reappraisal of an old tool for prolonged non-invasive modulation of brain excitability. Clin. Neurophysiol. 114, 589–595.

Priori, A., Mameli, F., Cogiamanian, F., Marceglia, S., Tiriticco, M., Mrakic-Sposta, S., Ferrucci, R., Zago, S., Polezzi, D., Sartori, G., 2008. Lie-specific involvement of dorsolateral prefrontal cortex in deception. Cereb. Cortex 18, 451–455.
Rigonatti, S.P., Boggio, P.S., Myczkowski, M.L., Otta, E., Fiquer, J.T., Ribeiro, R.B., Nitsche, M.A., Pascual-Leone, A., Fregni, F., 2008. Transcranial direct stimulation and fluoxetine for the treatment of depression. Eur. Psychiatry 23, 74–76.
Schlaug, G., Renga, V., 2008. Transcranial direct current stimulation: a noninvasive tool to facilitate stroke recovery. Expert Rev. Med. Devices 5, 759–768.
Smith, S.M., 2002. Fast robust automated brain extraction. Hum. Brain Mapp. 17, 143–155.
Stinear, C., 2010. Prediction of recovery of motor function after stroke. Lancet Neurol. 9, 1228–1232.
Wagner, T., Fregni, F., Fecteau, S., Grodzinsky, A., Zahn, M., Pascual-Leone, A., 2007. Transcranial direct current stimulation: a computer-based human model study. Neuroimage 35, 1113–1124.
Ward, N.S., Brown, M.M., Thompson, A.J., Frackowiak, R.S., 2003. Neural correlates of motor recovery after stroke: a longitudinal fMRI study. Brain 126, 2476–2496.
Williams, J.A., Imamura, M., Fregni, F., 2009. Updates on the use of non-invasive brain stimulation in physical and rehabilitation medicine. J. Rehabil. Med. 41, 305–311.
Woolrich, M., 2008. Robust group analysis using outlier inference. Neuroimage 41, 286–301.
Woolrich, M.W., Behrens, T.E., Beckmann, C.F., Jenkinson, M., Smith, S.M., 2004. Multilevel linear modelling for FMRI group analysis using Bayesian inference. Neuroimage 21, 1732–1747.